Analog Beamforming Enhancement for Field-of-View Extension of a 28 GHz OFDM Testbed

Adam Dubs, Nakyung Lee, and Sunwoo Kim
Department of Electronic Engineering, Hanyang University, South Korea
{duanandi16, nagyeong2379, remero}@hanyang.ac.kr

Abstract

In this paper, we explore the configurations of TMYTEK's BBox One and BBox Lite uniform rectangular array (URA) antennas. We place the transmit URA at specific locations and orientations to measure the power associated with distinct line-of-sight (LOS) angle-of-arrival (AoA) components under various analog combiner configurations. By customizing these analog combiner configurations, we extend the Field-of-View (FoV) from 90° to 120°. Furthermore, the proposed configurations improve AoA estimation accuracy, particularly when the transmitter is located near the edges of the FoV, compared to the default settings.

***Index Terms*—mmWave, Angle-of-Arrival, TMYTEK, Analog Beamforming**

I. Introduction

Since the advent of 5G communications, there has been increasing attention to beamforming and directional antennas for sensing [1]. A common uniform rectangular array (URA) antenna used by researchers in recent years is TMYTEK BBox One and BBox Lite [2], [3]. However, these URAs need careful beamforming to ensure accurate and precise angle-of-arrival (AoA) estimation as well as coverage. To this end, we propose a custom configuration method for the BBox One to extend the Field-of-View (FoV) and to increase AoA estimation accuracy throughout the FoV.

II. System Model

For our system model, we simplify the 4x4 URA to a four element uniform linear array (ULA) by only considering the horizontal components. Thus, the received signal model for the n-th OFDM symbol and the j-th beam at the RX can be written as follows:

$$\mathbf{y}_{\mathrm{j}}(n) = \alpha(n)\mathbf{w}_{\mathrm{j}}^{\mathrm{H}}\mathbf{a}(\theta_{AoA})\mathbf{x}(n) + \mathbf{n}_{\mathrm{j}}(n), \tag{1}$$

where $\mathbf{y}_{\mathrm{j}}(n)$ and $\mathbf{x}(n)$ represent the OFDM symbol time-domain complex data, $\mathbf{w}_{\mathrm{j}}$ is the combiner vector, $\mathbf{a}(\theta_{AoA})$ is the AoA steering vector, $\alpha(n)$ is the complex attenuation for the line-of-sight (LOS) path, and $\mathbf{n}_{\mathrm{j}}(n)$ is complex Gaussian white noise.

The steering vector is defined as

$$\mathbf{a}(\theta_{AoA}) = \begin{bmatrix} 1 & e^{j\beta} & e^{j2\beta} & e^{j3\beta} \end{bmatrix}^{\top}, \tag{2}$$

where $\beta = 2\pi d \sin(\theta_{AoA})/\lambda$. The distance between each antenna element, d, is 5 mm and the wavelength, λ, is about 10.7 mm. The combiner vector is defined similarly to the steering vector, but with each β, 2β, and 3β being manually configured.

III. Combiner Configuration

The analog combiner within the BBox One is configured using TMYTEK's general API [4]. There are two primary methods for configuring a specific beam: (1) specifying the main lobe direction, or (2) individually setting the phase of each antenna element. However, for method (1), the Field-of-View (FoV) is limited to within ±45°. Therefore, we extend the FoV of the receiver by manually configuring the antenna elements. From Eq. 1 and 2, it is clear that the maximum power of the received signal is when the exponents of the combiner equal the exponents of the steering vector. Therefore, for beam sweeping θ from -180° to 180°, β in the combiner is set to $2\pi d \sin(\theta)/\lambda$, converted to degrees, and rounded to the nearest multiple of 5.

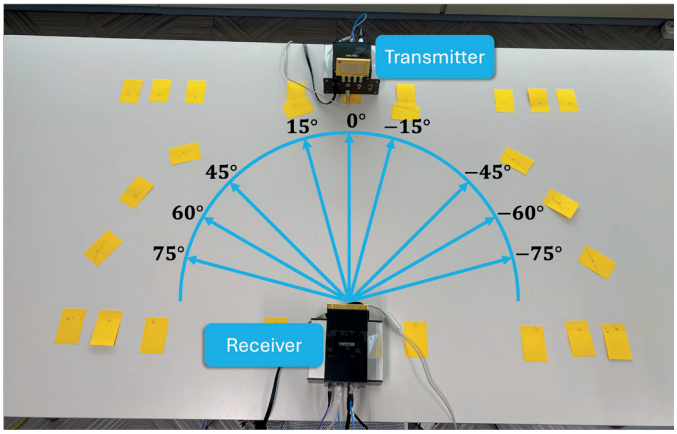

Fig. 1: Experiment setup

IV. Data Collection

The testbed proposed in [5] is used to sweep the beams and collect raw data. In Fig. 1, the experiment setup is shown with nine different locations for the transmitter. Because BBox One only allows for up to 64 unique beams to be defined, each beam sweep at one location is composed of multiple separate sweeps. For the proposed configuration, each complete sweep is composed of three separate sweeps from -90° to -31°, -30° to 30°, and 31° to 90° at 1° intervals. Likewise, the default configuration is swept twice with one sweep comprised of two

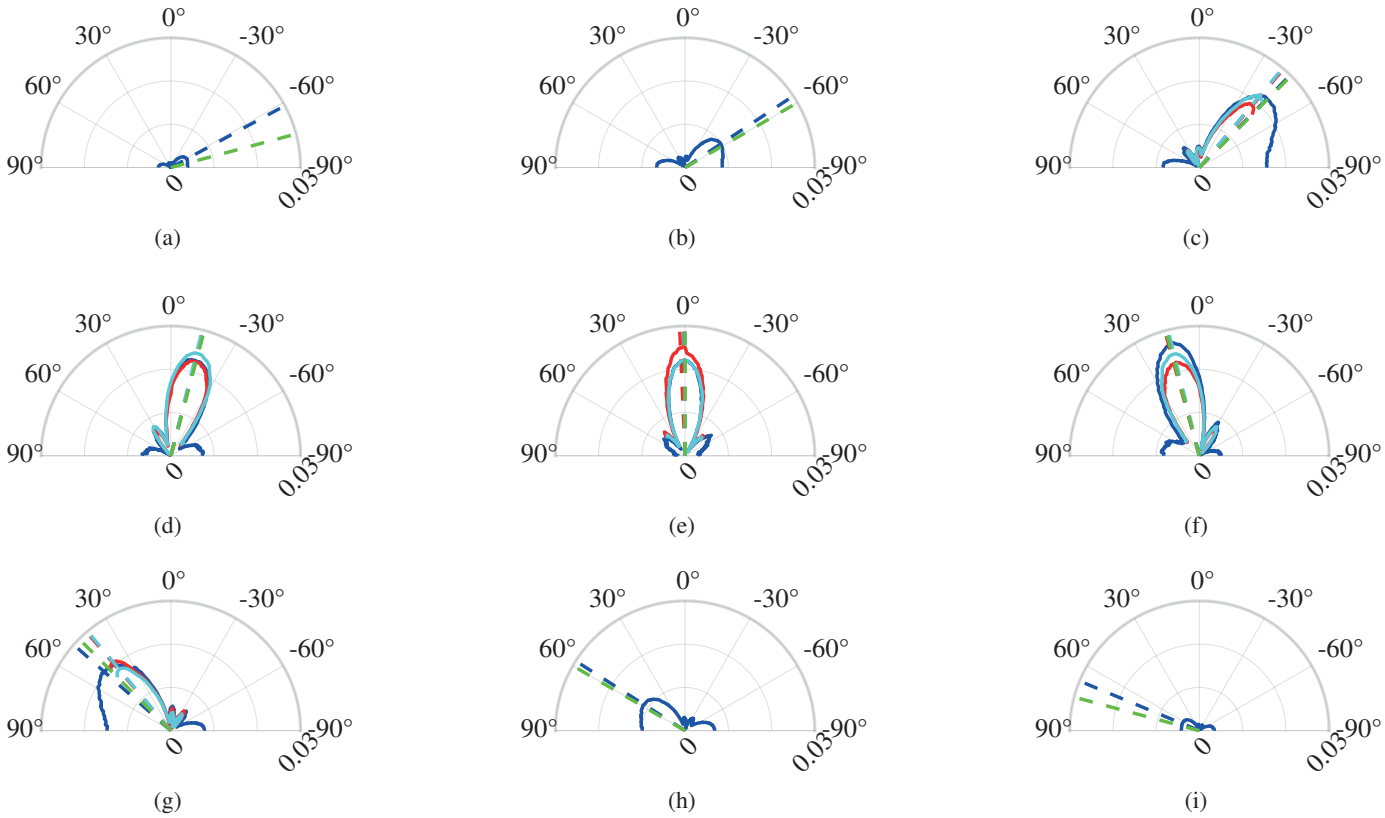

Fig. 2: Raw power measurements for each beam sweep are shown in (a)-(i), corresponding to transmitter placements in Fig. 1. The green dashed line indicates the ground truth. Blue lines show results and AoA estimates from the proposed configuration, red from the default configuration, and cyan from the default configuration sampled at 2° intervals.

separate sweeps from -45° to -1°and 0° to 45° at 1° intervals and the other sweep comprised of a single sweep from -45° to 45° at 2° intervals. From the raw data, the power is measured at each symbol boundary to ensure only the LOS components are measured. The power is then averaged over nine separate symbols. For estimating the AoA from the beam sweep data, a simple Bernstein estimator is used [6].

V. Analysis of Results

The results of the experiments are shown in Fig. 2. It is clear that the results for AoA estimation are not valid when the AoA is more than 60° away from the broadside as seen in Fig. 2a and 2i. However, for AoAs existing at ±60°, the estimation error was about 3° as shown in Fig. 2b and 2h. The differences between the default and proposed configurations can be seen in Fig. 2c-2g. Within ±30°, the configurations are mostly identical; therefore, the results in Fig. 2d, 2e and 2f show very little variation between the trials. However, outside ±30°, the default and proposed configurations diverge—especially in the 4th antenna's phase. As such, the average error is significantly different at ±45° as shown in Fig. 2c and 2g. The proposed configuration has an average error of about 2° whereas the default configuration has an average error of about 4.5°.

VI. Conclusions

In this paper, we explore the beam pattern for TMYTEK's BBox One and BBox Lite URAs under various proposed beam configurations. We demonstrate that the FoV can be expanded using our beam configurations. Furthermore, we show that AoA estimates are improved using our proposed beam configuration compared to the default settings at the edges of the FoV.

Acknowledgment

This work was supported by the National Research Foundation of Korea(NRF) grant funded by the Korea government(MSIT) (No. NRF-2023R1A2C3002890).

References

[1] F. Liu, Y. Cui, C. Masouros, J. Xu, T. X. Han, Y. C. Eldar, and S. Buzzi, "Integrated sensing and communications: Toward dual-functional wireless networks for 6G and beyond," *IEEE J. Sel. Areas Commun.*, vol. 40, no. 6, pp. 1728–1767, Jun. 2022.

[2] *Datasheet BBox One 5G 28 GHz BNE-2840-G*, TMYTEK, Oct. 2022. [Online]. Available: https://tmytek.com/resources/documents

[3] P. J. Gu, X. Li, V. C. Andrei, K. Vardanyan, U. J. Mönich, and H. Boche, "Very high-resolution sensing and communications testbed with 5G mmWave frontend," *2025 IEEE 5th Int. Symp. Joint Commun. & Sens.*, pp. 1–2, Jan. 2025.

[4] TMYTEK, "TLKCore," Feb. 2024, accessed: 2025-02-11. [Online]. Available: https://github.com/tmytek/tlkcore-examples/tree/dev/update-tlkcore-v120

[5] A. Dubs, H. Lee, S. Baek, and S. Kim, "WSL28: A 28 GHz OFDM bistatic radar testbed with an analog beamformer for AoA estimation," 2025, submitted for publication.

[6] M. A. Richards, J. A. Scheer, and W. L. Melvin, *Principles of Modern Radar: Basic Principles*, 1st ed. SciTech Publishing, 2010, vol. 1.